magnetochemistry

MDPI

Article

Critical Behavior of $La_{0.8}Ca_{0.2}Mn_{1-x}Co_xO_3$ Perovskite ($0.1 \leq x \leq 0.3$)

Dorra Turki [1], Zafar Khan Ghouri [2,*], Saeed Al-Meer [2,*], Khaled Elsaid [3], M. I. Ahmad [2], Ahmed Easa [2], Gyorgy Remenyi [4], Sami Mahmood [5], El Kebir Hlil [4], Mohamed Ellouze [6] and Foued Elhalouani [7]

1 Department of Chemistry and Earth Sciences, College of Arts and Sciences, Qatar University, P.O. Box 2713, Doha, Qatar; turki.dorra@qu.edu.qa
2 Central Laboratory Unit, Qatar University, P.O. Box 2713, Doha, Qatar; mohammad.ibrahim@qu.edu.qa (M.I.A.); ahmedaali@qu.edu.qa (A.E.)
3 Chemical Engineering Program, Texas A&M University at Qatar, P.O. Box 23874, Doha, Qatar; Khaled.elsaid@qatar.tamu.edu
4 Institut Néel, CNRS, Université Grenoble Alpes, 25 rue des Martyrs BP 166, 38042 Grenoble CEDEX 9, France; gyorgy.remenyi@neel.cnrs.fr (G.R.); el-kebir.hlil@neel.cnrs.fr (E.K.H.)
5 Department of Physics, The University of Jordan, Amman 11942, Jordan; s.mahmood@ju.edu.jo
6 Faculty of Sciences of Sfax, Department of Physics, University of Sfax, B.P. 1171, Sfax 3000, Tunisia; Mohamed.Ellouze@fss.rnu.tn
7 National Engineering School of Sfax, Department of Mechanical Engineering, University of Sfax, B.P.W, Sfax 3038, Tunisia; Foued.elhalouani@enis.rnu.tn
* Correspondence: zafarkhan.ghouri@qu.edu.qa or zafarkhanghouri@hotmail.com (Z.K.G.); salmeer@qu.edu.qa (S.A.-M.); Tel.:+974-50587742 (Z.K.G)

Received: 16 May 2017; Accepted: 8 September 2017; Published: 19 September 2017

Abstract: The critical properties of $La_{0.8}Ca_{0.2}Mn_{1-x}Co_xO_3$ (x = 0, 0.1, 0.2 and 0.3) compounds were investigated by analysis of the magnetic measurements in the vicinity of their critical temperature. Arrott plots revealed that the paramagnetic PM-ferromagnetic (FM) phase transition for the sample with x = 0 is a first order transition, while it is a second order transition for all doped compounds. The critical exponents β, γ and δ were evaluated using modified Arrott plots (MAP) and the Kouvel-Fisher method (KF). The reliability of the evaluated critical exponents was confirmed by the Widom scaling relation and the universal scaling hypothesis. The values of the critical exponents for the doped compounds were consistent with the 3D-Heisenberg model for magnetic interactions. For x = 0.1, the estimated critical components are found inconsistent with any known universality class. In addition, the local exponent n was determined from the magnetic entropy change and found to be sensitive to the magnetic field in the entire studied temperature range.

Keywords: manganites; critical behavior; critical exponents; local exponents

1. Introduction

Several investigations had been carried out on the sensitivity of the physical properties of manganites to the substitution of Mn cations at B-sites by trivalent and tetravalent ions such as Fe, Co, Mo and Cr [1–4]. These physical properties were explained by various phenomena such as the double exchange (DE) model [5,6], phase separation [7], Jahn-Teller distortion [8,9] and the Griffiths-like phase (GP) [10]. The competition between antiferromagnetic (AFM) and ferromagnetic (FM) interactions, as well as magnetic inhomogeneity and disorder leads to magnetic short-range order in transition metal-doped manganites [11].

Since the values of critical exponents play an important role in elucidating the interaction mechanisms near the Curie temperature (T_C) and identifying the universality class of the material,

several studies focused on investigating the critical behavior of manganites in the vicinity of T_C [12,13]. Generally, the discontinuous ferromagnetic-paramagnetic FM-PM transition at T_C as a consequence of structural changes is a first-order magnetic transition (FOMT) [14–16]. This discontinuous phase transition can evolve into a continuous second-order magnetic phase transition (SOMT) upon doping the manganite [17].

Critical behavior in the DE model was first described within the long-range mean field theory [18,19]. Afterwards, Motomeand Furukawa suggested that the critical behavior should be attributed to the short-range Heisenberg model [20,21]. However, significant differences in the critical exponents and universality of manganites were found in the literature. Specifically, previous studies on $La_{0.8}Ca_{0.2}MnO_3$-based materials indicated FOMT and/or second-order magnetic transition (SOMT) [22,23]. Consequently, an in-depth investigation of the critical behavior of each synthesized manganite compound is essential for understanding and interpreting its magnetic behavior in terms of intrinsic parameters and basic interactions. Accordingly, we were motivated to investigate the critical behavior and universality class in a series of Co-doped ($La_{0.8}Ca_{0.2}Mn_{1-x}Co_xO_3$). To achieve a deeper insight, analysis of the field dependence of the magnetic entropy change using the power law $|\Delta S_{max}(H)| \infty H^n$ [24,25] was carried out, and the results were compared with the results of the study of the critical behavior.

2. Experimental Details

$La_{0.8}Ca_{0.2}Mn_{1-x}Co_xO_3$ samples (x = 0.1, 0.2 and 0.3) were synthesized using the sol-gel method. Appropriate proportions of La_2O_3, CaO, MnO_2 and Co_3O_4 powders (99% purity) were used for the synthesis of the precursor powders of the manganites. The precursor powders were pressed into pellets and calcined at 1000 °C for 3 h. X-ray diffraction was used to check the structural phases and phase purity of the samples, where all compounds were found to crystallize in an orthorhombic structure with the Pnma space group. The Magnetization measurements were carried out using the BS1 magnetometer developed at Neel institute Laboratory in Grenoble. Isothermal magnetization *M (H)* data were measured in the temperature range 5 K–300 K under an applied field *H* varying from 0–5 T.

3. Results and Discussion

Figure 1 Shows XRD patterns, while the refined cell parameters for all of the samples are listed in the table (inset Figure 1). The variations in cell parameters were previously discussed in terms of the differences in ionic radii of Mn^{3+} and Co^{3+} ions and internal stress induced by Co substitution [26]. The ionic radius of Mn^{3+} (0.645 Å) is higher than that of Co^{3+} (0.61 Å); consequently, it was estimated that the Co doping results in a decrease in the lattice parameters and volume. However, contrary to expectations, increasing the Co content up to x = 0.2 results in an increase in cell volume, then a slight decrease was observed in the sample with x = 0.3 (table inset of Figure 1). This sharp deviation can be ascribed to the distortion mesh-induced substitution of Mn by Co, as evidenced by the fluctuations of the angles (B-O-B) and length (B-O) of ionic bonds of cobalt or manganese with oxygen ions [27]. For the non-doped compound, FM DE interactions are more dominant than AFM interactions of Mn^{3+}-$Mn^{3+}$and Mn^{4+}-Mn^{4+}, and the presence of Co favours AFM SE interactions. Since Co replaces Mn, which causes the increase of the Mn^{3+}/Mn^{4+}ratio, the level of hopping electrons and the number of available hopping sites decrease. The DE interaction is thus suppressed, resulting in the reduction of ferromagnetism when Co content increases and so the decrease of both T_C and magnetization.

Figure 2 shows the SEM images of the prepared sample. All of the images of the samples show particles having aspherical shape, and most of them connect with each other. Corresponding EDX analysis (insets Figure 2) revealed the presence of La, Ca, Mn, O and Co elements.

In a previous work [26], we reported that the PM-FM transition in $La_{0.8}Ca_{0.2}Mn_{1-x}Co_xO_3$ compounds occurs at 256 K and 176 K for x = 0 and x = 0.2, respectively. For the sample with x = 0, the existence of the Griffiths phase was reported, as well.

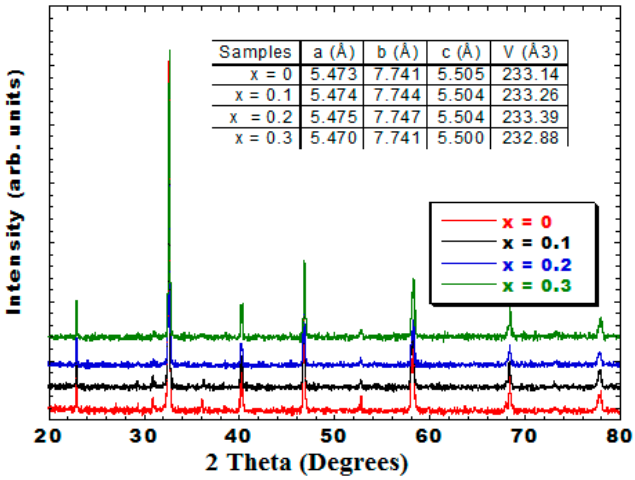

Figure 1. XRD patterns for $La_{0.8}Ca_{0.2}Mn_{1-x}Co_xO_3$ (x = 0, 0.1, 0.2, 0.3). Inset table: cell parameters.

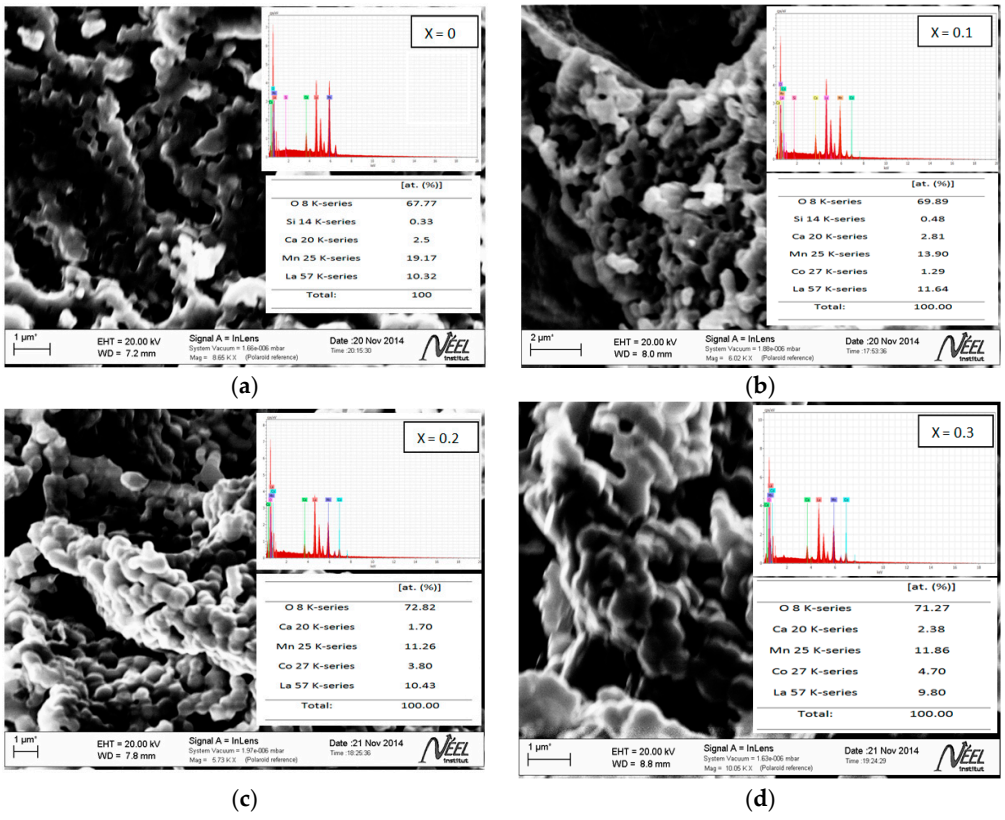

Figure 2. SEM micrographs, EDX and deduced atomic composition of corresponding samples. (**a**) $La_{0.8}Ca_{0.2}MnO_3$; (**b**) $La_{0.8}Ca_{0.2}Mn_{0.9}Co_{0.1}O_3$; (**c**) $La_{0.8}Ca_{0.2}Mn_{0.8}Co_{0.2}O_3$; and (**d**) $La_{0.8}Ca_{0.2}Mn_{0.7}Co_{0.3}O_3$.

Figure 3 shows the isothermal magnetization curves for $La_{0.8}Ca_{0.2}Mn_{1-x}Co_xO_3$ (x = 0, 0.1, 0.2 and 0.3). The *H*/*M* vs. M^2 Arrott plots displayed in Figure 4wereanalyzed using the Banerjee criterion [28] to determine the type of magnetic phase transition in these samples. According to this criterion, $La_{0.8}Ca_{0.2}MnO_3$ nanopowder exhibited negative slopes, indicating that this sample is characterized by a first-order magnetic transition (FOMT) (Figure 4 x = 0). However Zhang et al. [15] reported second-order magnetic transition (SOMT). The same composition was prepared by Khlifi et al. [29] using the solid state reaction at two different annealing temperatures and found to be FOMT at 1073 K and SOMT at 1473 K. Similarly, Phan et al. [16] reported FOMT in $La_{0.7}Ca_{0.3}MnO_3$ manganite. Lynn et al. [30]

conclude that $La_{0.7}Ca_{0.3}MnO_3$ manganite does not exhibit a continuous second-order phase transition. This observation is also confirmed by Lin et al. [31] when they clarify the breakdown of critical scaling in $La_{0.7}Ca_{0.3}MnO_3$ owing to a transition that is not an ordinary second-order ferromagnetic transition. Recently, Bonilla et al. [32] observed a breakdown of the universal behaviour for $La_{2/3}Ca_{1/3}MnO_3$, which is a sign of the first-order nature of the phase. With Co doping, the PM-FM phase transition is changed from first order to second order. As reported by Kim et al. [33] the critical exponents cannot be defined for the first-order ferromagnetic phase transition, because the magnetic field induces a shift in the transition temperature, leading to a field-dependent phase boundary near T_C. However, the second-order magnetic phase transition near the Curie point is characterized by a set of critical exponents, β (associated with the spontaneous magnetization), γ (relevant to the initial magnetic susceptibility) and δ (associated with the critical magnetization isotherm). The nature of the magnetic phase transition in $La_{0.8}Ca_{0.2}Mn_{1-x}Co_xO_3$ samples with x = 0.1, 0.2 and 0.3 was investigated by evaluating their critical exponents near T_C. The critical exponents were determined from the commonly-known modified Arrott plots (MAP) based on the Arrott–Noakes equation of state [34]:

$$\left(\frac{H}{M}\right)^{1/\gamma} = \frac{T - Tc}{T_1} + \left(\frac{M}{M_1}\right)^{1/\beta} \quad (1)$$

where T_1 and M_1 are some constantsthatare characteristic of the material.

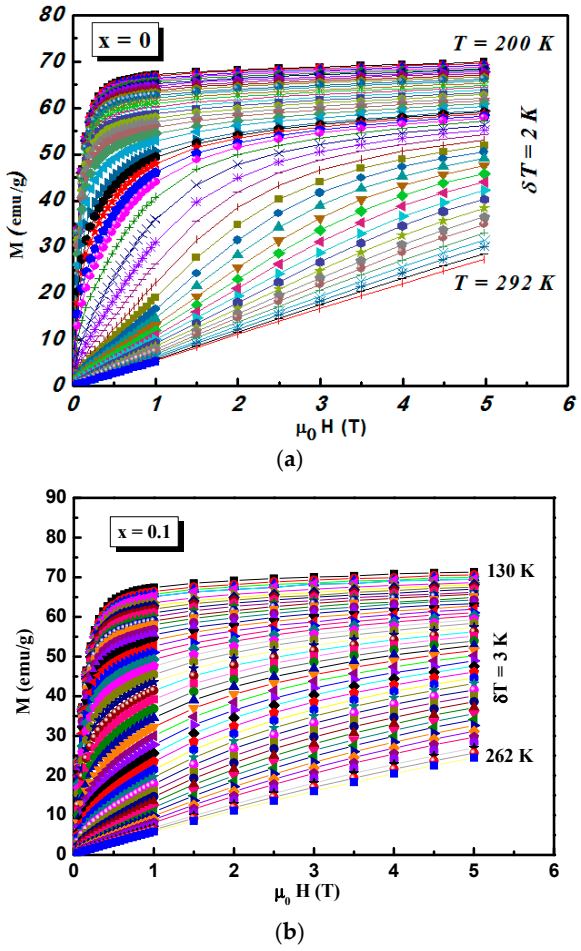

Figure 3. *Cont.*

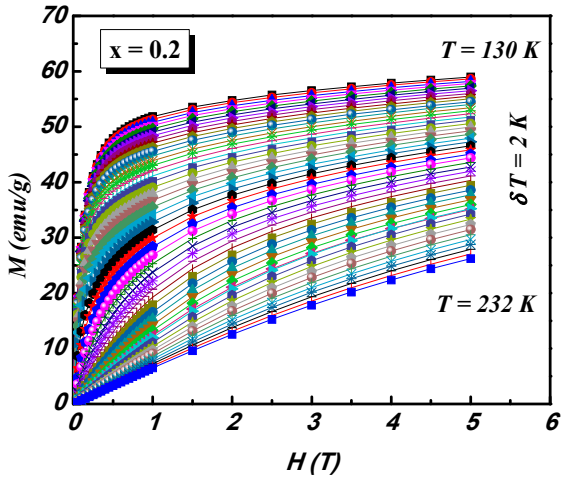

(**c**)

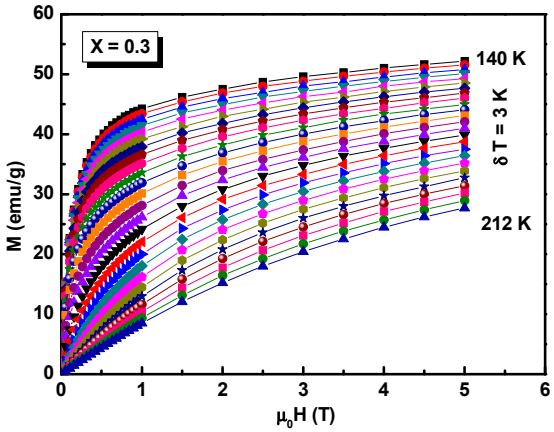

(**d**)

Figure 3. Magnetization vs. applied magnetic field $\mu_0 H$ measured at different temperatures for: (**a**) $La_{0.8}Ca_{0.2}MnO_3$; (**b**) $La_{0.8}Ca_{0.2}Mn_{0.9}Co_{0.1}O_3$; (**c**) $La_{0.8}Ca_{0.2}Mn_{0.8}Co_{0.2}O_3$; and (**d**) $La_{0.8}Ca_{0.2}Mn_{0.7}Co_{0.3}O_3$.

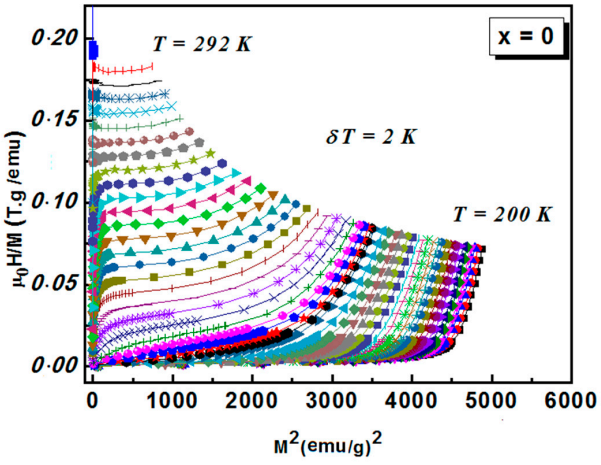

(**a**)

Figure 4. *Cont.*

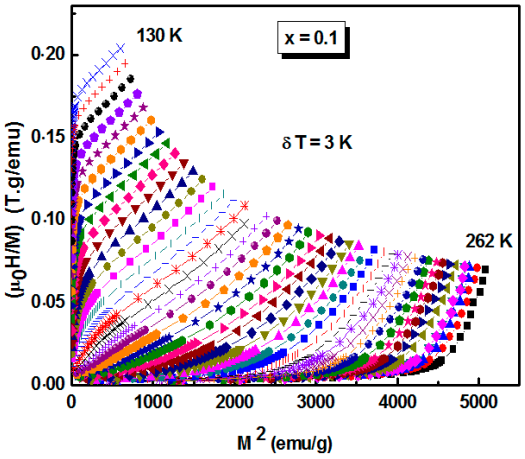

(**b**)

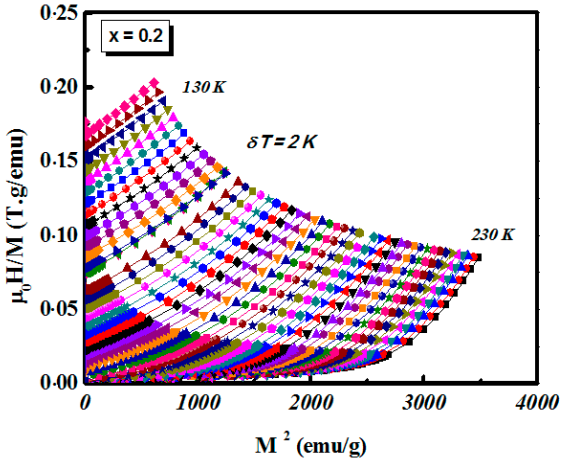

(**c**)

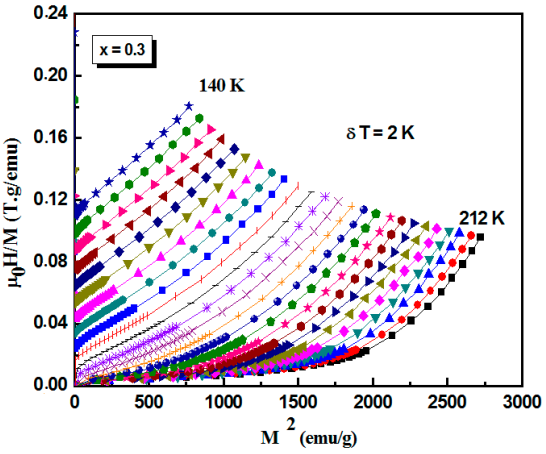

(**d**)

Figure 4. Arrott plots *H*/*M* vs. M^2 plot for $La_{0.8}Ca_{0.2}Mn_{1-x}Co_xO_3$. (**a**) x = 0; (**b**) x = 0.1; (**c**) x = 0.2; and (**d**) x = 0.3.

Figure 5 shows the modified Arrot tplots $M^{1/\beta}$ vs. $(H/M)^{1/\gamma}$ using four different values of trial exponents corresponding to mean field theory ($\beta = 0.5$, $\gamma = 1$), the 3D-Heisenberg model ($\beta = 0.365$, $\gamma = 1.336$), the 3D-Ising model ($\beta = 0.325$, $\gamma = 1.241$) and the tricritical mean-field model ($\beta = 0.25$, $\gamma = 1$).

The critical exponents corresponding to the appropriate model that best describes magnetic interactions in a material should give quasi-straight lines that are nearly parallel in the high magnetic field region at temperatures around T_C. The MAPs in Figure 5 clearly indicate that the long-range mean-field model and the 3D-Ising model are inappropriate to describe magnetic interactions in the samples under investigation. To determine which of the other two models is the most appropriate, the relative slope RS = S(T)/S(T_C) in the high-field region was evaluated at different temperatures around T_C and presented in Figure 6. For a series of perfectly parallel straight lines in the modified Arrott plots, one should obtain a constant value of one for RS, irrespective of temperatures [35]. According to this criterion, the 3D-Heisenberg model turned out to be the model that best describes the magnetic interactions in all doped samples as demonstrated by Figure 6.

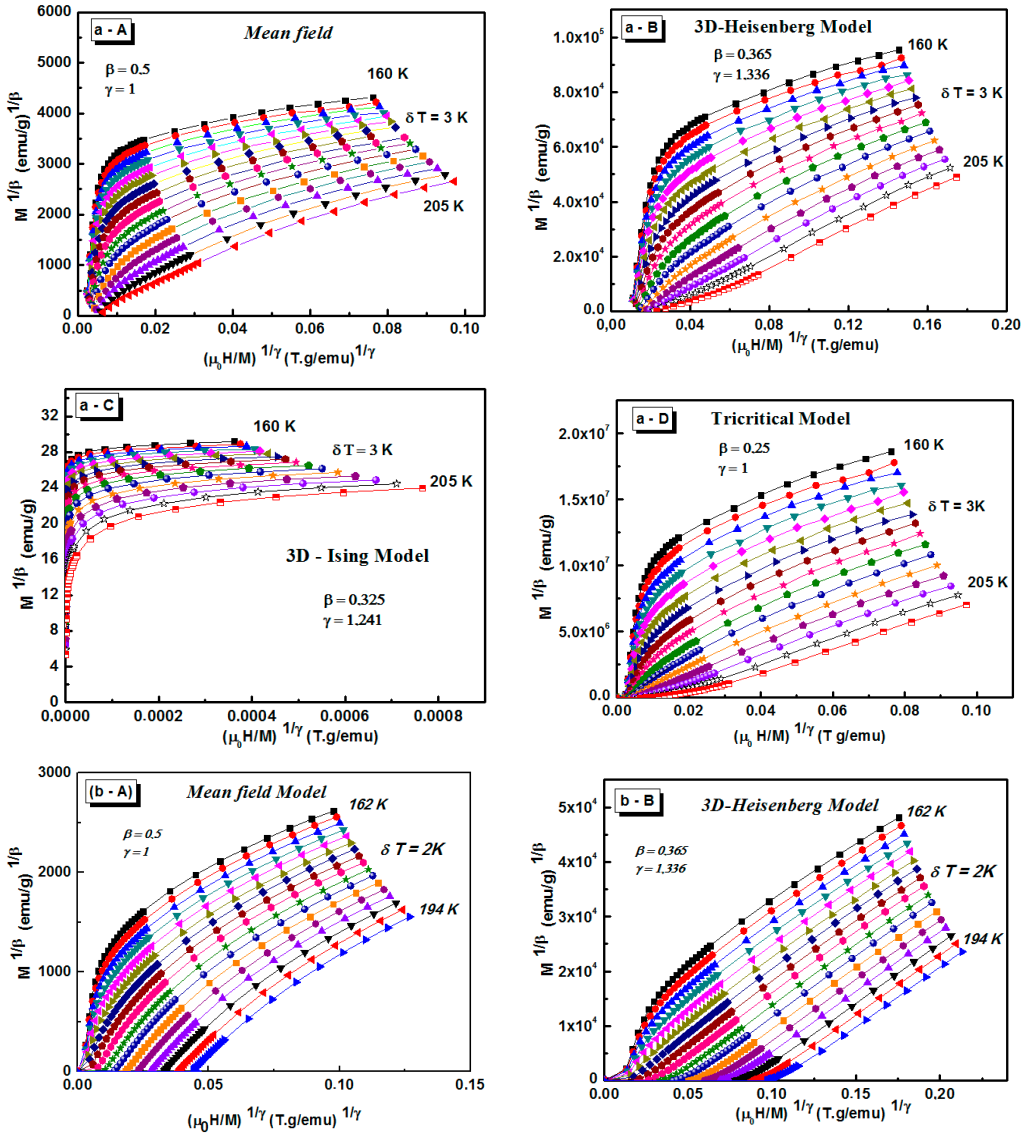

Figure 5. *Cont.*

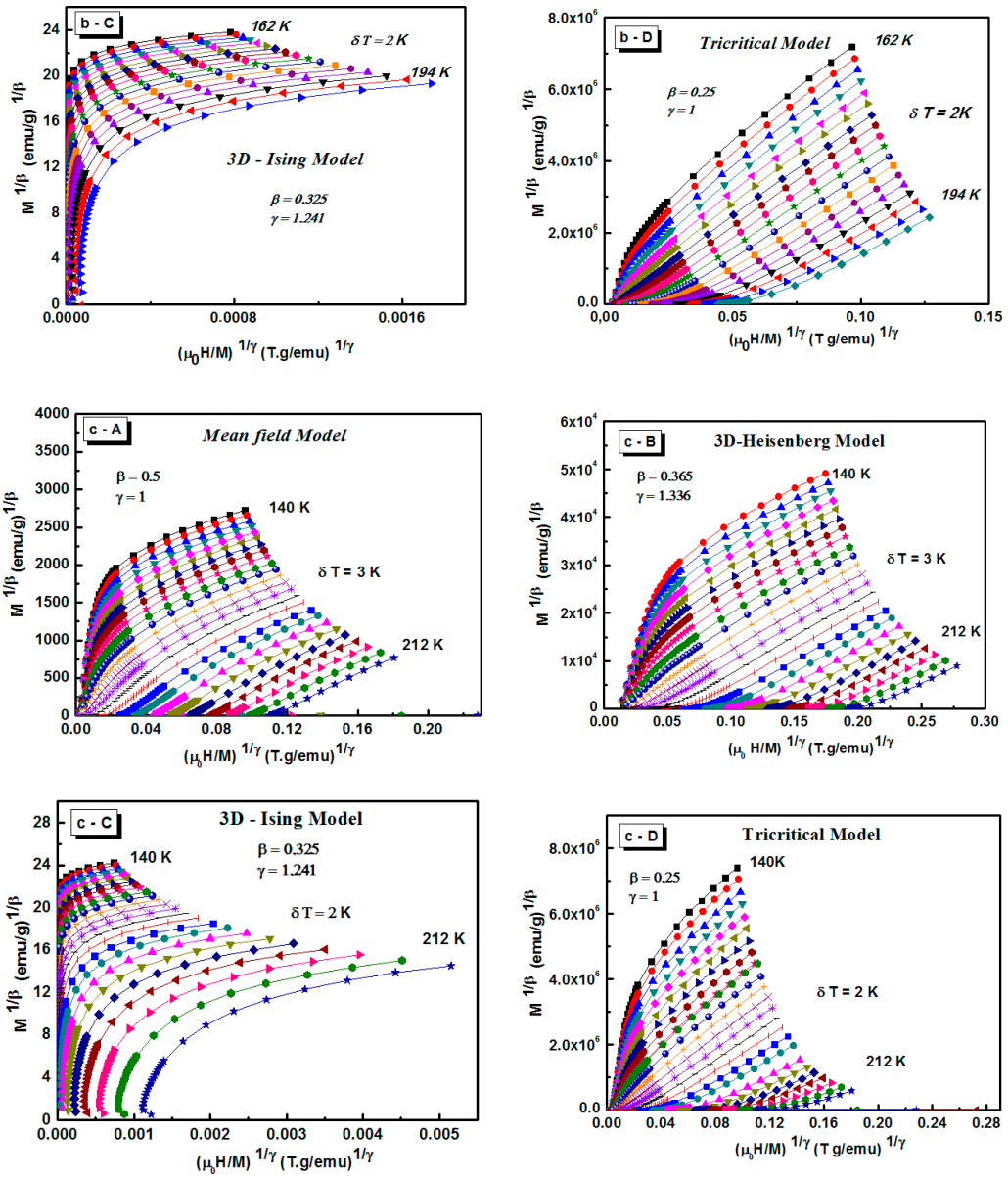

Figure 5. (**A**) Arrott plots M^2 vs. (H/M); (**B**–**D**) isotherms of $M^{1/\beta}$ vs. $(H/M)^{1/\gamma}$ for the modified Arrott plots; (**B**) 3D-Heisenberg model ($\beta = 0.365$, $\gamma = 1.336$); (**C**) 3D-Ising ($\beta = 0.325$, $\gamma = 1.241$); and (**D**) tricritical mean field ($\beta = 0.25$, $\gamma = 1$); for $La_{0.8}Ca_{0.2}Mn_{1-x}Co_xO_3$: (**a**) x = 0.1, (**b**) x = 0.2 and (**c**) x = 0.3.

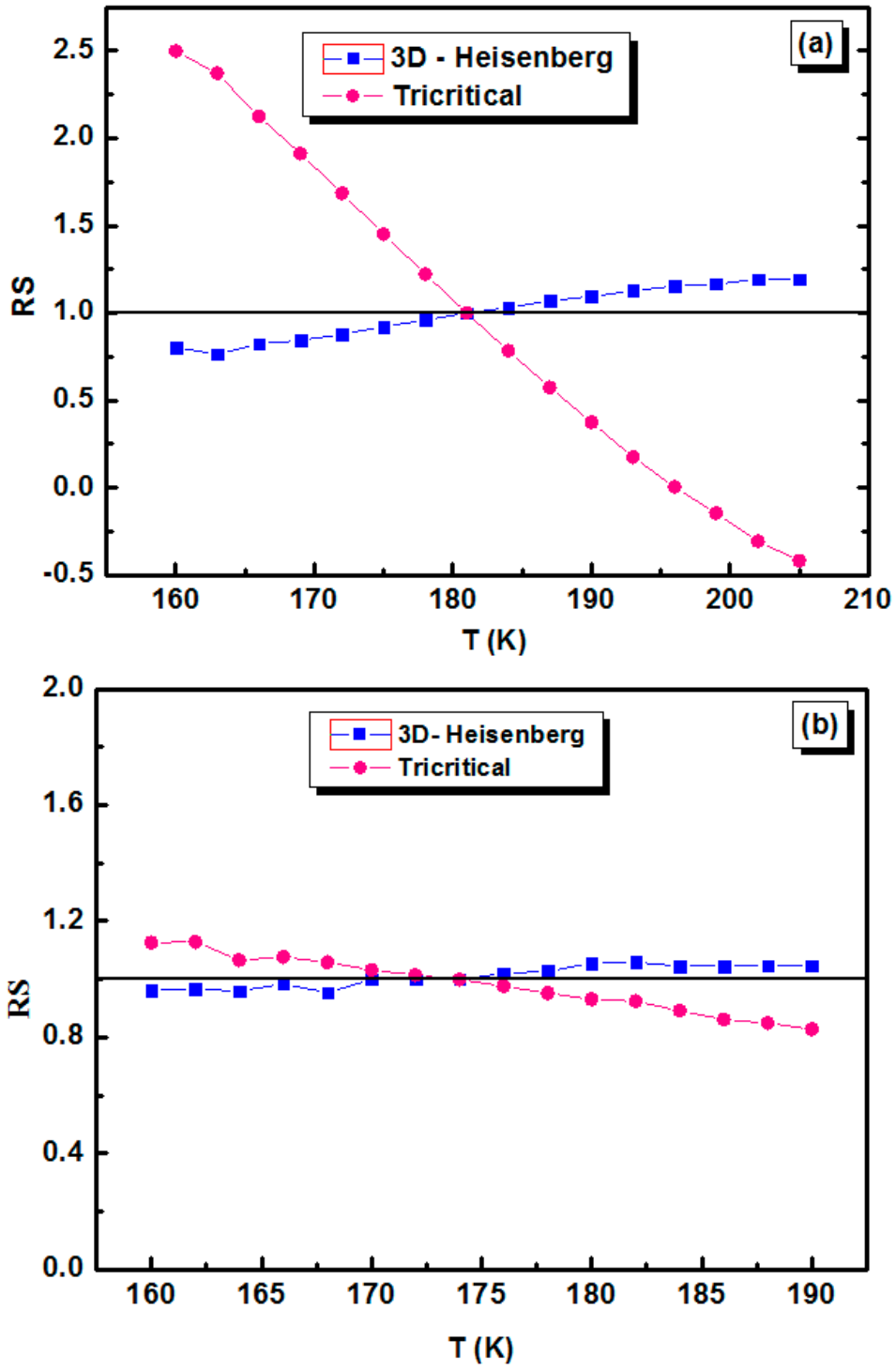

Figure 6. *Cont.*

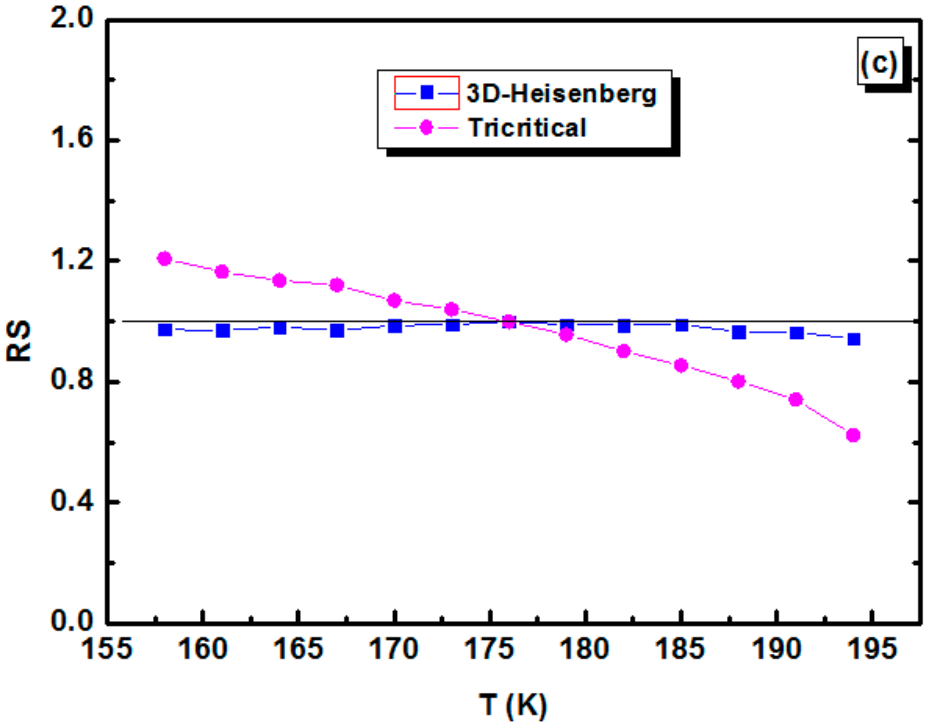

Figure 6. Relative slope (RS) as a function of temperature, defined as RS = S(T)/S(T_C), RS being the experimental slopes at high fields, for $La_{0.8}Ca_{0.2}Mn_{1-x}Co_xO_3$. (**a**) x = 0.1; (**b**) x = 0.2; and (**c**) x = 0.3.

The values of the spontaneous magnetization $M_S(T)$ and ${\chi_0}^{-1}(T)$ are obtained by extrapolating the linear parts of the MAPs in the high-magnetic field region to intersect the $M^{1/\beta}$ and the $(H/M)^{1/\gamma}$ axes, respectively. According to the scaling hypothesis, the temperature dependences of the spontaneous magnetization (M_S) and inverse initial susceptibility (${\chi_0}^{-1}$) obey the asymptotic relations.

$$M_S(T) = M_0(-\varepsilon)^{\beta}, \varepsilon < 0, \tag{2}$$

$$\chi_0^{-1}(T) = (h_0/M_0)\varepsilon^{\gamma}, \varepsilon > 0, \tag{3}$$

$$M = DH^{1/\delta}, \varepsilon = 0, \tag{4}$$

where $\varepsilon = (T - T_C)/T_C$ is the reduced temperature and M_0, h_0 and D are the critical amplitudes. Here, β, γ and δ are the critical exponents characteristic of FM short-range order or long-range order, depending on their values. More accurately, the critical exponents can be also obtained from the Kouvel–Fisher (KF) method [36] using the following equations:

$$\frac{M_S(T)}{dM_S(T)/dT} = \frac{T - T_C}{\beta} \tag{5}$$

$$\frac{x_0^{-1}(T)}{dx_0^{-1}(T)/dT} = \frac{T - T_C}{\gamma} \tag{6}$$

This method suggests that the curves of $M_S(T)$ $(dM_S(T)/dT)^{-1}$ and ${\chi_0}^{-1}(T)(d{\chi_0}^{-1}$ $(T)/dT)^{-1}$ plotted versus temperature should yield straight lines with slopes $(1/\beta)$ and $(1/\gamma)$, respectively, and the intercepts of the T axis give T_C.

Figure 7 shows the spontaneous magnetization *Ms*(*T*) as a function of temperature and fitted using Equations (2) and (5). This fitting gives values of β and T_C. The values obtained by fitting the curves of the samples with x = 0.1, 0.2 and 0.3 are, respectively: (β_{MAP} = 0.204 ± 0.06 with T_C = 188.271 K and

β_{KF} = 0.123 ± 0.04 with T_C = 182.384 K), (β_{MAP} = 0.401 ± 0.02 with T_C = 176.32 K and β_{KF} = 0.418 ± 0.04 with T_C = 176.34 K) and (β_{MAP} = 0.333 ± 0.03 with T_C = 172.61 K and β_{KF} = 0.404 ± 0.01 with T_C = 174.35 K).

Figure 8 shows the inverse initial susceptibility χ_0^{-1} (T) as a function of temperature. Least-squares fitting of the straight lines gave the following values of γ and T_C for the samples with x = 0.1, 0.2 and 0.3, respectively: (γ_{MAP} = 1.969 ± 0.01 with T_C = 153.72 K and γ_{KF} = 1.351 ± 0.08 with T_C = 166.655 K); (γ_{MAP} = 1.332 ± 0.05 with T_C = 175.21 K and γ_{KF} = 1.303 ±0.01 with T_C = 175.14 K) and (γ_{MAP} = 1.298 ± 0.02 with T_C = 171.59 K and γ_{KF} = 1.27 ± 0.04 with T_C = 171.89 K).

These results show that the obtained critical exponents for the sample with x = 0.2 are consistent with the 3D-Heisenberg exponents. However, the exponents for the sample with x = 0.3 are between 3D-Ising and 3D-Heisenberg exponents. The evaluated exponents for x = 0.1 are inconsistent with any known universality class, and the convergence was reached with different values of transition temperature T_C. It can be clearly seen that the values of T_C for x = 0.1 and 0.3 deviate from that obtained by magnetic measurement at 5 K (Table 1) [19]. This deviation is generally due to the incomplete polarization of spins [37].

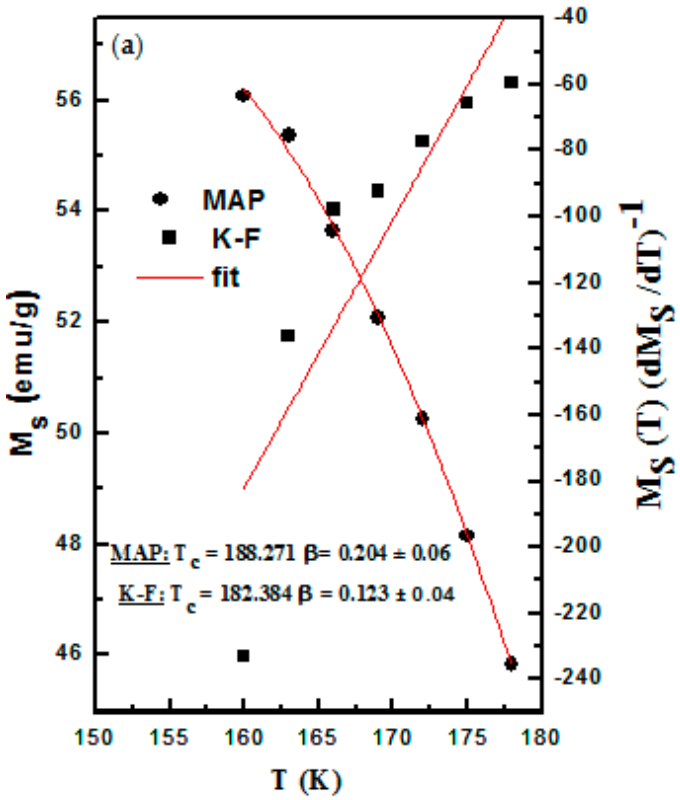

Figure 7. *Cont.*

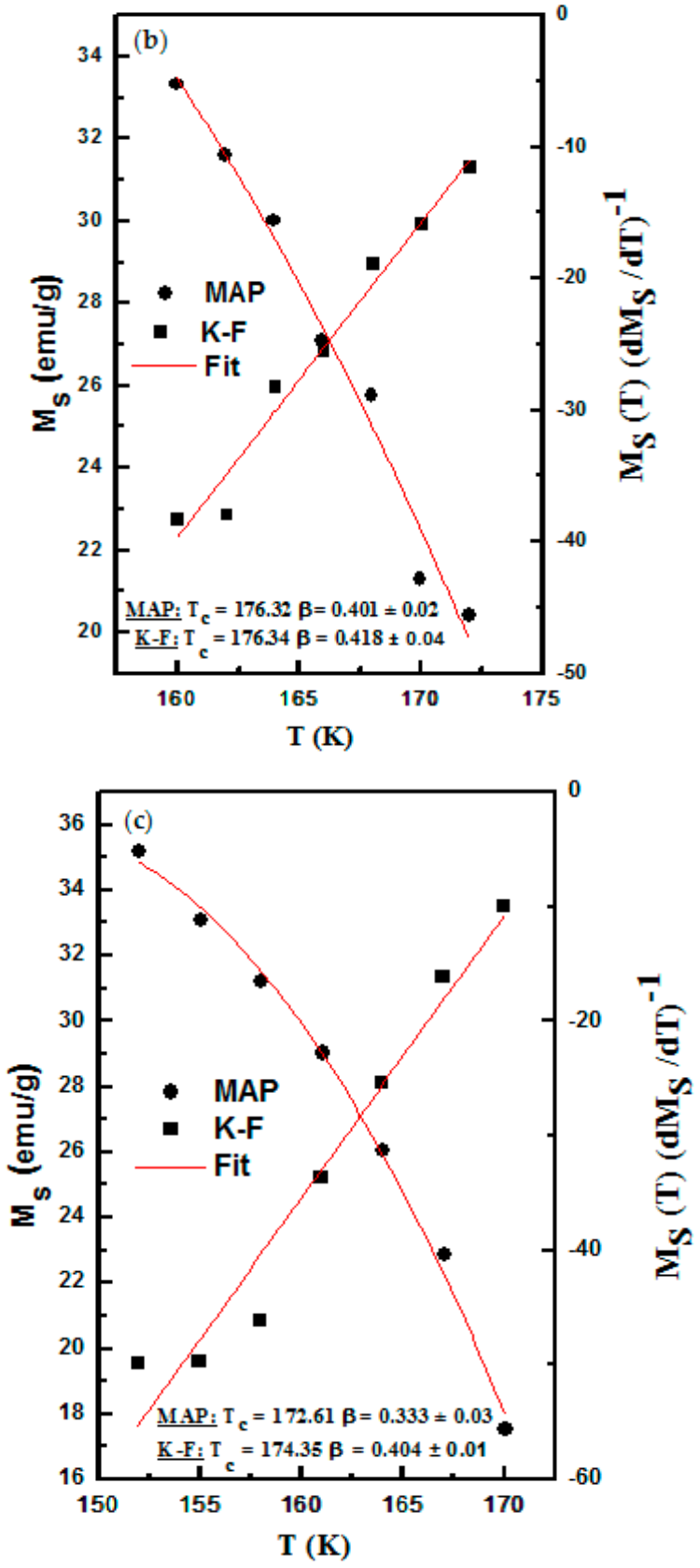

Figure 7. The spontaneous magnetization *Ms* (*T*) as a function of temperature, along with fits (solid curves) based on the power laws (left-axis) defined by (2) and Kouvel–Fisher (right-axis) defined by Equation (5), respectively. For $La_{0.8}Ca_{0.2}Mn_{1-x}Co_xO_3$, (**a**) x = 0.1, (**b**) x = 0.2, (**c**) x = 0.3.

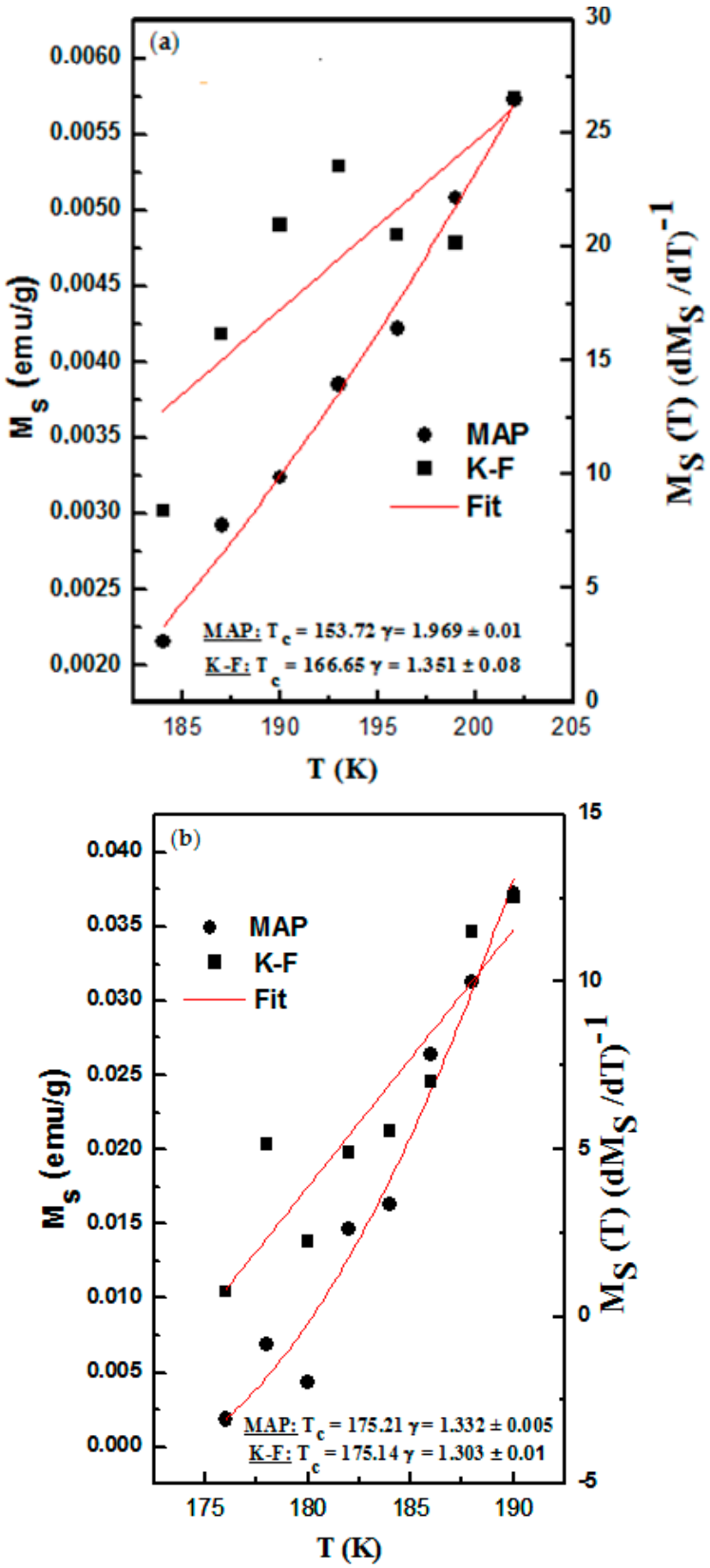

Figure 8. *Cont.*

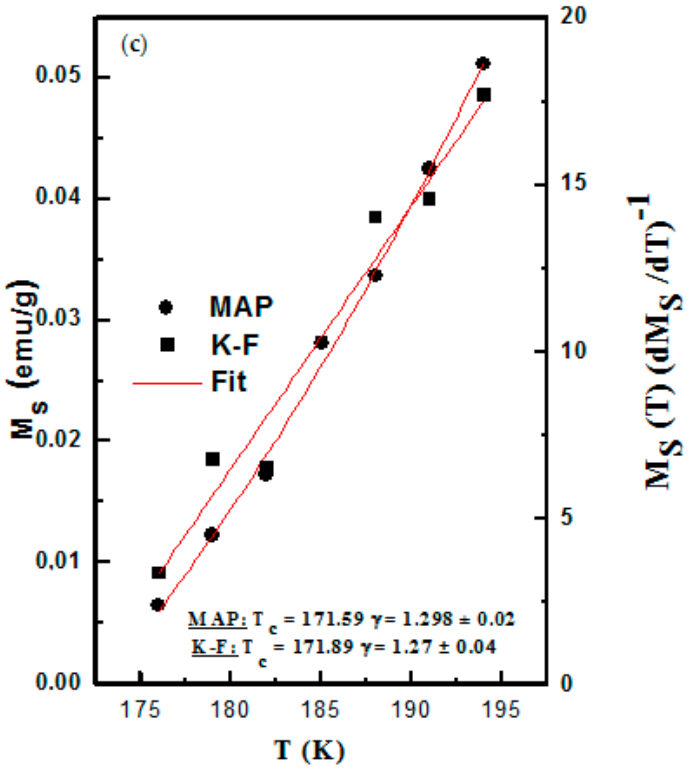

Figure 8. The inverse initial susceptibility $\chi_0{}^{-1}$(T) as a function of temperature, along with fits (solid curves) based on the power laws (left-axis) defined by (3) and Kouvel-Fisher (right-axis) defined by Equation (6), respectively. For $La_{0.8}Ca_{0.2}Mn_{1-x}Co_xO_3$, (**a**) x = 0.1, (**b**) x = 0.2, (**c**) x = 0.3.

Table 1. Comparison of critical exponents for $La_{0.8}Ca_{0.2}Mn_{1-x}Co_xO_3$ compounds with earlier reports, Abbreviations: MAP, modified Arrott plot; KF, Kouvel-Fisher method; CI, critical Isotherm; exp, experimental; cal, calculated.

Compositions	Model	T_C(K)	β	γ	δ	Ref.
Mean-field model	Theory	-	0.5	1	3	[28]
3D-Heisenberg model	Theory	-	0.365 ± 0.003	1.386 ± 0.004	4.8	[28]
3D-Ising model	Theory	-	0.325 ± 0.003	1.241 ± 0.002	4.82	[28]
Tricritical mean field model	Theory	-	0.25	1	5	[28]
$La_{0.8}Ca_{0.2}Mn_{0.9}Co_{0.1}O_3$	MAP	188.3	0.204 ± 0.06	1.969 ± 0.01	11.983	This Work
	KF method	182.4	0.123 ± 0.04	1.351 ± 0.08		
	CI (exp)	181	-	-	7.51	
$La_{0.8}Ca_{0.2}Mn_{0.8}Co_{0.2}O_3$	MAP	176.3	0.401 ± 0.02	1.332 ± 0.05	4.321	This Work
	KF method	176.3	0.418 ± 0.04	1.303 ± 0.01		
	CI (exp)	176	-	-	4.081	
$La_{0.8}Ca_{0.2}Mn_{0.7}Co_{0.3}O_3$	MAP	172.6	0.333 ± 0.03	1.298 ± 0.02	4.897	This Work
	KF method	174.3	0.404 ± 0.01	1.27 ± 0.04		
	CI (exp)	173	-	-	4.629	
$La_{0.8}Ca_{0.2}MnO_3$ (0–1T)	-	185.6	0.349 ± 0.013	1.231 ± 0.03	4.524	[15]
$La_{0.8}Ca_{0.2}MnO_3$ (1–2T)	-	188.5	0.316 ± 0.007	1.081 ± 0.036	4.421	
$La_{0.8}Ca_{0.2}MnO_3$ (2–3T)	-	190.4	0.281 ± 0.009	0.992 ± 0.036	4.534	
$La_{0.8}Ca_{0.2}MnO_3$ (3–4T)	-	194.0	0.272 ± 0.006	0.910 ± 0.021	4.341	
$La_{0.8}Ca_{0.2}MnO_3$ (4–5T)	-	195.3	0.259 ± 0.004	0.918 ± 0.036	4.552	
$La_{0.8}Ca_{0.2}MnO_3$	MAP	181.375	0.328	1.193	-	[23]
	KF method	181.676	0.325	1.180	-	
	CI (exp)	-	-	-	4.826	
	CI (cal)	-	-	-	4.630	
$Pr_{0.73}Ca_{0.27}MnO_3$	-	127	0.36	1.36	4.81	[37]

Table 1. *Cont.*

Compositions	Model	T_C(K)	β	γ	δ	Ref.
$La_{0.9}Te_{0.1}MnO_3$	-	240	0.201	1.27	7.14	[38]
$La_{0.77}Ca_{0.23}MnO_3$	-	185	0.43	1.35	5.5	[39]
$La_{0.75}Ca_{0.25}MnO_3$	-	189	0.51	1.15	15	
$La_{0.7}Sr_{0.3}MnO_3$	KF	360	0.3776 ± 0.004	1.1686 ± 0.006	4.106 ± 0.01	[40]
$La_{0.7}Sr_{0.3}Mn_{0.95}Co_{0.05}O_3$	KF	320	0.4036 ± 0.005	1.1596 ± 0.007	3.886 ± 0.01	
$La_{0.7}Sr_{0.3}Mn_{0.9}Co_{0.1}O_3$	KF	281	0.4576 ± 0.007	1.1146 ± 0.005	3.446 ± 0.01	
$La_{0.7}Sr_{0.3}Mn_{0.85}Co_{0.15}O_3$	KF	274	0.4186 ± 0.004	1.1876 ± 0.006	3.846 ± 0.01	
$La_{0.7}Sr_{0.3}CoO_3$	KF	224	0.4146 ± 0.007	1.2086 ± 0.008	3.926 ± 0.01	
$La_{0.7}Sr_{0.3}Mn_{0.95}Co_{0.05}O_3$	-	360	0.387 ± 0.008	1.166 ± 0.01	4 4.01	[11]
$La_{0.7}Sr_{0.3}Mn_{0.94}Co_{0.06}O_3$	-	311	0.478 ± 0.013	1.165 ± 0.027	3.44	
$La_{0.7}Sr_{0.3}Mn_{0.92}Co_{0.08}O_3$	-	297	0.483 ± 0.018	1.112 ± 0.028	3.30	
$La_{0.7}Sr_{0.3}Mn_{0.9}Co_{0.1}O_3$	-	281	0.487 ± 0.016	1.109 ± 0.063	3.28	
$Nd_{0.7}Sr_{0.3}MnO_3$	-	240	0.271	0.922	-	[41]
$(Nd_{0.93}Y_{0.07})_{0.7}Sr_{0.3}MnO_3$	-	175	0.234–0.236	1.044–1.063	-	
$(La_{0.9}Dy_{0.1})_{0.8}Pb_{0.2}MnO_3$	-	248.4	0.484 ± 0.02	0.961 ± 0.012	2.90 ± 0.01	[42]
$La_{0.79}Ca_{0.21}MnO_3$	-	182	0.09	1.71	20	[43]

The third critical exponent δ is directly obtained by fitting the high field region of the critical isotherm $M(T_C,H)$ plotted on a log-log scale (Supplementary, Figure S1). The value of the third critical exponent evaluated in this manner was then compared with that calculated from the Widom scaling relation [44]:

$$\delta = 1 + \frac{\gamma}{\beta} \tag{7}$$

The values of critical exponents for our samples are listed in Table 1 and compared with some other reported values in the literature. In fact, δ(cal) obtained from Equation (7) is close to δ(CI) deduced from the critical isotherm for x = 0.2 and 0.3. However, for x = 0.1, we found that δ(CI) = 7.51 is close to that obtained for $La_{0,9}Te_{0,1}MnO_3$ (δ(CI) = 7.14) [38], and δ(cal) = 11.983 is close to δ(cal)= 15 obtained for $La_{0.75}Ca_{0.25}MnO_3$ [39].

Assessing the reliability of the critical parameters can be carried out by means of the scaling hypothesis [45], which predicts that in the asymptotic critical region, the magnetic equation of state can be expressed as:

$$M(H,\varepsilon) = |\varepsilon|^{\beta} f_{\pm}\left(H/|\varepsilon|^{\beta+\gamma}\right) \tag{8}$$

where $f_{\pm}$ are regular functions with f_+ for $T > T_C$ and f_- for $T < T_C$. It means that plotting $M/|\varepsilon|^{\beta}$ vs. $H/|\varepsilon|^{\beta+\gamma}$ makes all high-field data points fall into two universal branches corresponding to $T > T_C$ and $T < T_C$. Using the values of β and γ obtained by the MAP (the case of x = 0.2 and 0.3) and both MAP and KF for x = 0.1 (to check the validity of the exponents), the scaled data are plotted in Figure 9. The inset shows the same plots in a log-log scale. It is found that experimental data for x = 0.2 and 0.3 fall on two independent branches even in a low field region, indicating that the obtained values of critical exponents are reasonable for the description of magnetic interactions in these samples. Nevertheless, the critical exponents exhibited by the sample $La_{0.8}Ca_{0.2}Mn_{0.9}Co_{0.1}O_3$ are obviously anomalous and do not belong to any universality class previously reported, indicating that the ferromagnetic transition in this system is unconventional. In fact, in highly-disordered systems, the critical exponents are found to be almost abnormal and do not belong to any class of universality [12,46]. Similar results have been deduced for $La_{0.7}Sr_{0.3}Mn_{1-x}Co_xO_3$ [40]. Phan et al. [11] demonstrated that the substitution of Co dopants dilutes the Mn lattice and changes the disorder of the Mn-related magnetic lattice. Furthermore, they concluded that with the same composition, critical exponent values are dependent on the sample type (single-crystal or polycrystalline form), and on the nature of dopants and the concentration. Additionally, the doped site (A or B-site), as well as the type of atoms also affect the values of critical temperature and critical exponents and a precise determination of the type of magnetic transition becomes difficult when the magnetic transition is a mixture of FOMT and SOMT [41,42,46]. Moreover, several studies show that the presence of FM cluster in manganites can also modify the critical exponents [47,48].

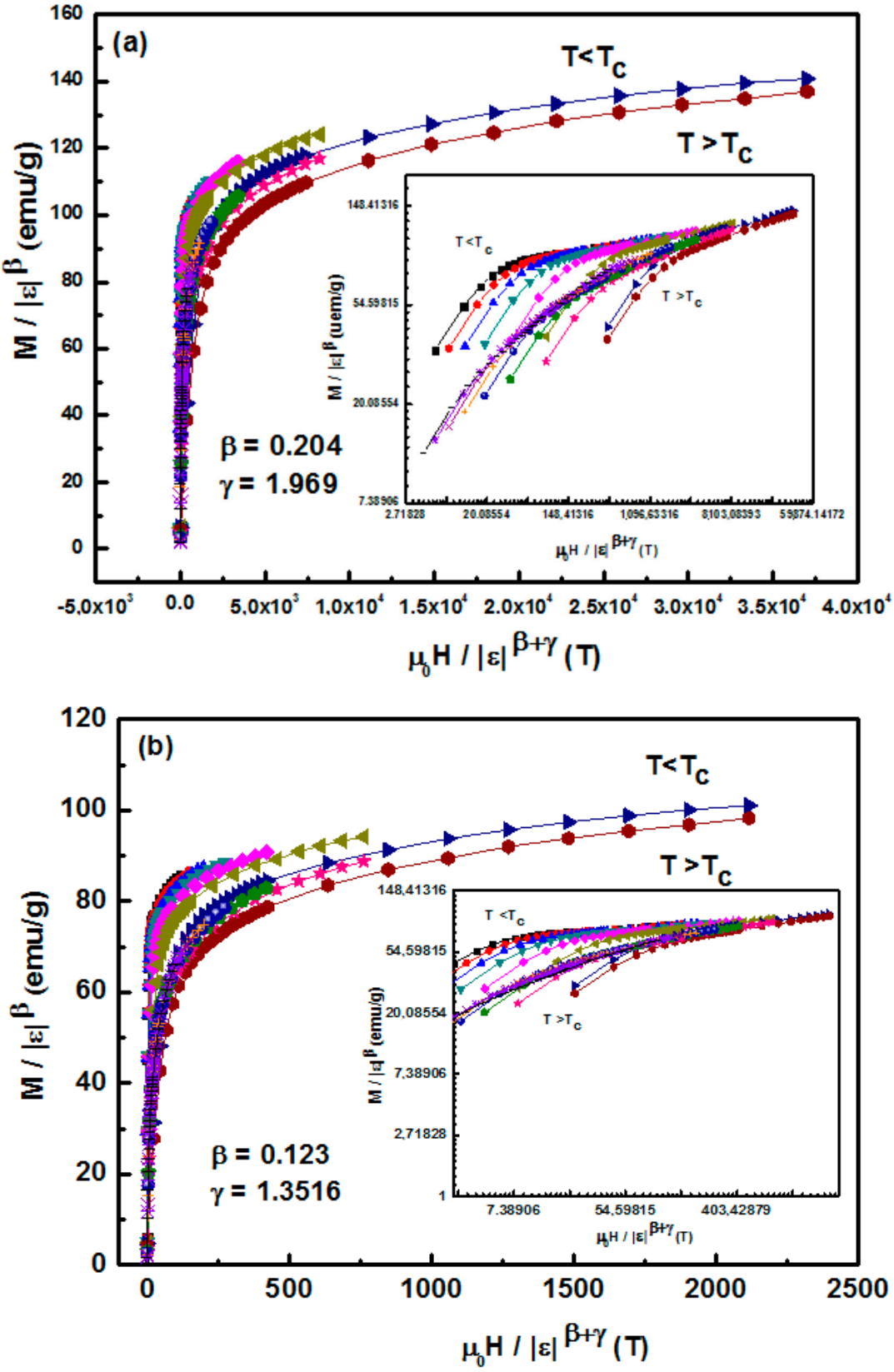

Figure 9. *Cont.*

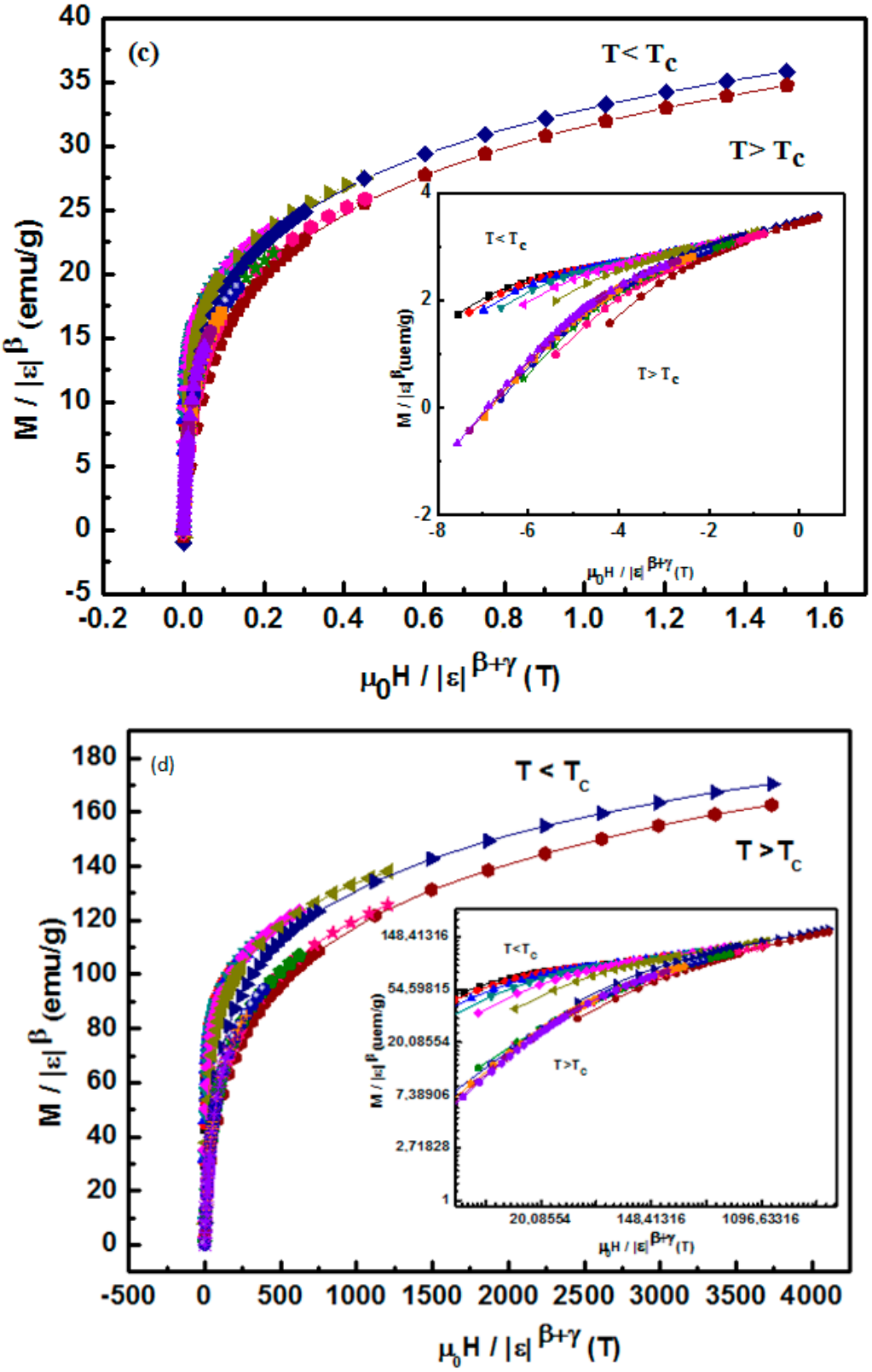

Figure 9. Scaling plots below and above T_C using β and γ determined from the modified Arrott plots. The inset shows the same plots on a log-log scale. For $La_{0.8}Ca_{0.2}Mn_{1-x}Co_xO_3$, (**a**) x = 0.1 with β = 0.204 and γ = 1.969; (**b**) x = 0.1 with β = 0.123 and γ = 1.3516; (**c**) x = 0.2; and (**d**) x = 0.3.

The field dependence of the entropy change related to the local exponent n has been analyzed using the results of magnetic entropy change. Indeed, according to Oesterreicher et al. [24], the field dependence of the magnetic entropy change of materials with a second-order phase transition is expressed as:

$$|\Delta S_{max}(H)| \infty H^n \tag{9}$$

where the exponent n depends on the magnetic state of the compound (Supplementary, Figure S2). Moreover, it can be locally calculated as follows:

$$n = \frac{dln\,|\Delta S_M|}{dlnH} \tag{10}$$

Some authors claim that second-order phase transitions materials should be represented by the mean field model with the corresponding $n = 2/3$ [24], and any deviation from that value should be explained by the distribution of the Curie temperatures of the material [49,50]. Using the power law (Equation (9)) represented in Supplementary Figure S2, the obtained values of n are 0.833, 0.731 and 0.845 for x = 0.1, 0.2 and 0.3, respectively. These values deviate significantly from the mean field predictions [36]. From Figure 10, it can be clearly seen that n evolves with the field in the entire studied temperature range and exhibits minimum values around their peak temperatures [51,52].

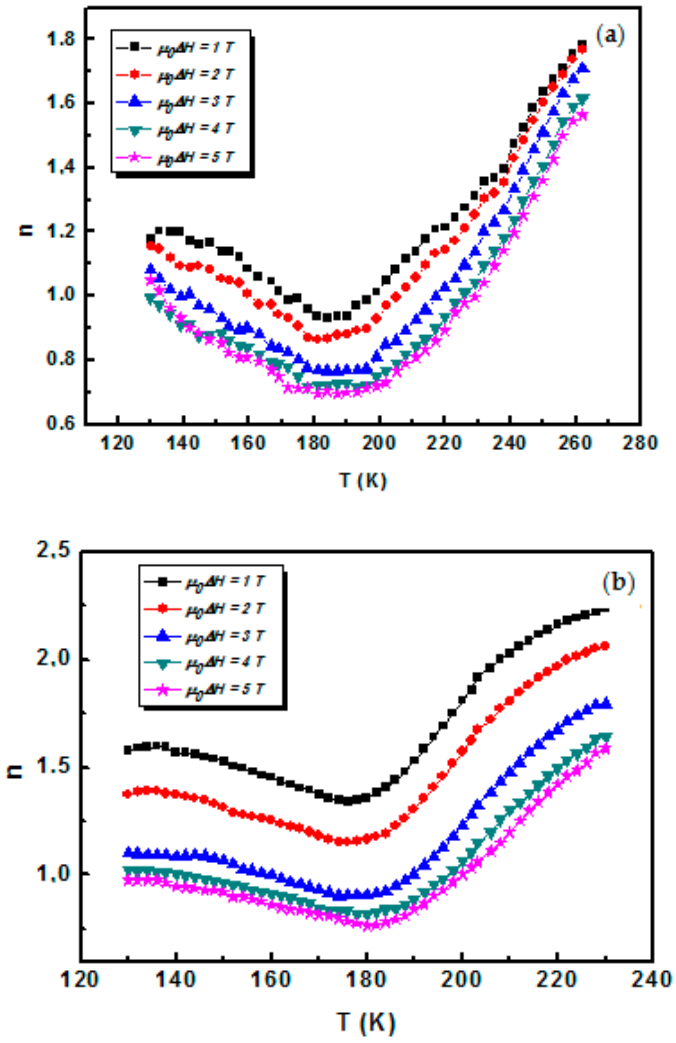

Figure 10. *Cont.*

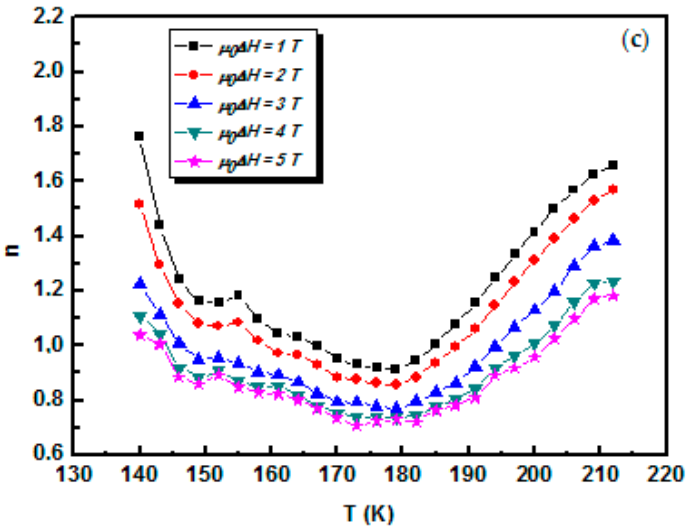

Figure 10. Temperature dependence of local exponent n measured at different field for $La_{0.8}Ca_{0.2}Mn_{1-x}Co_xO_3$. (**a**) x = 0.1; (**b**) x = 0.2; (**c**) x = 0.3.

The value of n obtained for x = 0.2 is in the vicinity of the value n = 0.75, being close to that obtained for the soft magnetic amorphous alloys [53,54].

In addition, we calculated n from the critical exponent β and γ using the relation [25]:

$$n\ (T_c) = 1 + \frac{\beta - 1}{\beta + \gamma} \tag{11}$$

Using Equation (7), Relation (11) can be rewritten as:

$$n\ (T_c) = 1 + \frac{1}{\delta}\left(1 - \frac{1}{\beta}\right) \tag{12}$$

The exponents n are calculated using Equation (11) or (12). The obtained values are 0.405, 0.654 and 0.591 for x = 0.1, 0.2 and 0.3, respectively. These values are lower than those deduced from the power law. We believe that a large deviation of the n values obtained from two routes is because the exponent values β and γ are much different from those expected for mean field theory, especially for x = 0.1. Thus, the variation of $n(T,H)$ indicates the inhomogeneous character of our compounds, although the presence of a minority magnetic phase would alter the value of the magnetic entropy change exponent. In this context, Shen et al. [55] show that in single-phase materials, n is field independent especially at the temperature corresponding to the minimum of n. In a multi-phase system or a system with magnetic inhomogeneity, $n(T)$ is field dependent at any temperature. Caballero et al. [56] studied the critical behavior of $Pr_{0.5}Sr_{0.5}MnO_3$ and concluded that for small applied magnetic fields, the magnetic field response of magnetization is weak in materials exhibiting FM clusters, thus resulting in a small change in magnetic entropy, while for high applied magnetic fields, all of the magnetic moments are aligned with the magnetic field resulting in an overall change in magnetic entropy that is close to the theoretically predicted value. In short, the local exponent n gives further insight into the critical behavior in the compound.

4. Conclusions

We have investigated the critical behavior of $La_{0.8}Ca_{0.2}Mn_{1-x}Co_xO_3$ (x = 0.1, 0.2, 0.3) samples around the PM-FM phase transition. This transition is identified to be second-order. The critical exponents β, γ and δ were evaluated from various techniques such as modified Arrott plots, the Kouvel-Fisher method and critical isotherm analysis. The estimated critical exponents for

$La_{0.8}Ca_{0.2}Mn_{0.9}Co_{0.1}O_3$ indicate that the ferromagnetic transition belongs to a new universality class. For x = 0.2 and 0.3, the estimated critical exponents are consistent with those of the short-range 3D-Heisenberg model. Accordingly, the significant decrease of T_C with the decrease in saturation magnetization for this sample influenced the values of the critical exponents, but without affecting the dimension of the order parameter (n = 3).The field dependence of the magnetic entropy change is also analyzed. It has been shown that n increase with the field in the whole studied temperature range. The obtained values of n using the power law are higher than those calculated using critical exponents. We consider that this large deviation of the n values obtained from the two methods is because the exponent values β and γ are much different from those expected for mean field theory. To conclude, the critical behaviour of manganites depends on the concentration and nature of the dopants.

Supplementary Materials: The following are available online at www.mdpi.com/2312-7481/3/3/28/s1, Figure S1: Linear fit of isothermal magnetic curves at $T = T_C$ = 181 K, 176 K and 173 K for $La_{0.8}Ca_{0.2}Mn_{1-x}Co_xO_3$ with x = 0.1, 0.2 and 0.3, respectively, Figure S2: Linear fit of magnetic entropy change curves at T_C = 181 K, 176 K and 173 K for $La_{0.8}Ca_{0.2}Mn_{1-x}Co_xO_3$ with x = 0.1, 0.2 and 0.3, respectively.

Acknowledgments: This work has been supported by the Tunisian Ministry of Scientific Research and Technology and Institute Neel at Grenoble.

Author Contributions: Dorra Turki, Zafar Khan Ghouri, Saeed Al-Meer, Khaled Elsaid, M. I. Ahmad and Ahmed Easa conceived the idea and designs the experiment. Data analysis is done by Gyorgy Remenyi, Zafar Khan Ghouri, Sami Mahmood, El Kebir Hlil, Mohamed Ellouze and Foued Elhalouani. Dorra Turki and Zafar Khan Ghouri wrote the manuscript while all authors contributed to the discussions.

Conflicts of Interest: The authors declare no conflict of interest.

References

1. Abdelkhalek, S.B.; Kallel, N.; Kallel, S.; Pena, O.; Oumezzine, M. Critical behavior and magnetic entropy change in the $La_{0.6}Sr_{0.4}Mn_{0.8}Fe_{0.1}Cr_{0.1}O_3$ perovskite. *J. Magn. Magn. Mater.* **2012**, *324*, 3615–3619. [CrossRef]
2. Nasri, M.; Triki, M.; Dhahri, E.; Hlil, E.K. Critical behavior in Sr-doped manganites $La_{0.6}Ca_{0.4-x}Sr_xMnO_3$. *J. Magn. Magn. Mater.* **2013**, *324*, 806. [CrossRef]
3. Chen, L.; He, J.H.; Mei, Y.; Cao, Y.Z.; Xia, W.W.; Xu, H.F.; Zhu, Z.W.; Xu, Z. Critical behavior of Mo-doping $La_{0.67}Sr_{0.33}Mn_{1-x}Mo_xO_3$ perovskite system. *Phys. B Condens. Matter* **2009**, *404*, 1879–1882. [CrossRef]
4. Oumezzine, M.; Pena, O.; Kallel, S.; Oumezzine, M. Crossover of the magnetocaloric effect and its importance on the determination of the critical behaviour in the $La_{0.67}Ba_{0.33}Mn_{0.9}Cr_{0.1}O_3$ perovskite manganite. *J. Alloys Compd.* **2012**, *539*, 116–123. [CrossRef]
5. Zener, C. Interaction between the *d*-Shells in the Transition Metals. II. Ferromagnetic Compounds of Manganese with Perovskite Structure. *Phys. Rev.* **1951**, *82*, 403. [CrossRef]
6. Anderson, P.W.; Hasegawa, H. Considerations on Double Exchange. *Phys. Rev.* **1955**, *100*, 675. [CrossRef]
7. Burgy, J.; Dagotto, E.; Mayr, M. Percolative transitions with first-order characteristics in the context of colossal magnetoresistance manganites. *Phys. Rev. B* **2003**, *67*, 014410. [CrossRef]
8. Millis, A.J.; Littlewood, P.B.; Shraiman, B.I. Double Exchange Alone Does Not Explain the Resistivity of $La_{1-x}Sr_xMnO_3$. *Phys. Rev. Lett.* **1995**, *74*, 5144. [CrossRef] [PubMed]
9. Millis, A.J.; Shraiman, B.I.; Mueller, R. Dynamic Jahn-Teller Effect and Colossal Magnetoresistance in $La_{1-x}Sr_xMnO_3$. *Phys. Rev. Lett.* **1996**, *77*, 175. [CrossRef] [PubMed]
10. Salamon, M.B.; Lin, P.; Chun, S.H. Colossal Magnetoresistance is a Griffiths Singularity. *Phys. Rev. Lett.* **2002**, *88*, 197203. [CrossRef] [PubMed]
11. Phan, T.-L.; Thanh, T.D.; Yu, S.C. Influence of Co doping on the critical behavior of $La_{0.7}Sr_{0.3}Mn_{1-x}Co_xO_3$. *J. Alloys Compd.* **2014**, *615*, S247–S251. [CrossRef]
12. Triki, M.; Dhahri, E.; Hlil, E.K. Unconventional critical magnetic behavior in the Griffiths ferromagnet $La_{0.4}Ca_{0.6}MnO_{2.8\Delta0.2}$oxide. *J. Solid State Chem.* **2013**, *201*, 63–67. [CrossRef]
13. Gdaiem, M.A.; Abassi, M.; Dhahri, J.; Hlil, E.K. Structural, magnetic, magnetocaloric properties and the formation of nano-size Griffiths-like clusters in $La_{0.8}Ba_{0.1}Ca_{0.1}Mn_{0.8}Co_{0.2}O_3$ manganites. *J. Alloys Compd.* **2015**, *646*, 1068–1074. [CrossRef]
14. Mira, J.; Rivsa, J.; Rivadulla, F.; Vazquez, C.V.; Quintela, M.A.L. Change from first- to second-order magnetic phase transition in $La_{2/3}(Ca,Sr)_{1/3}MnO_3$ perovskites. *Phys. Rev. B* **1999**, *60*, 2998.

15. Zhang, P.; Lampen, P.; Phan, T.L.; Yu, S.C.; Thanh, T.D.; Dan, N.H.; Lam, V.D.; Srikanth, H.; Phan, M.H. Influence of magneticfield on critical behavior near afirst order transition in optimally doped manganites: The case of $La_{1-x}Ca_xMnO_3$ ($0.2 < x < 0.4$). *J. Magn. Magn. Mater.* **2013**, *348*, 146–153.
16. Phan, M.H.; Franco, V.; Bingham, N.S.; Srikanth, H.; Hur, N.H.; Yu, S.C. Tricritical point and critical exponents of $La_{0.7}Ca_{0.3-x}Sr_xMnO_3$ (x = 0, 0.05, 0.1, 0.2, 0.25) single crystals. *J. Alloys Compd.* **2010**, *508*, 238–244. [CrossRef]
17. Phan, T.-L.; Tran, Q.T.; Thanh, P.Q.; Yen, P.D.H.; Thanh, T.D.; Yu, S.C. Critical behavior of $La_{0.7}Ca_{0.3}Mn_{1-x}Ni_xO_3$ manganites exhibiting the crossover of first-and second-order phase transitions. *Solid State Commun.* **2014**, *184*, 40–46. [CrossRef]
18. Seeger, M.; Kaul, S.N.; Kronmuller, H.; Reisser, R. Asymptotic critical behavior of Ni. *Phys. Rev. B* **1995**, *51*, 12585. [CrossRef]
19. Kubo, K.; Ohata, N. A Quantum Theory of Double Exchange. *J. Phys. Soc. Jpn.* **1972**, *33*, 21–32. [CrossRef]
20. Motome, Y.; Furulawa, N. Critical Temperature of Ferromagnetic Transition in Three-Dimensional Double-Exchange Models. *J. Phys. Soc. Jpn.* **2000**, *69*, 3785–3788. [CrossRef]
21. Motome, Y.; Furulawa, N. Critical Phenomena of Ferromagnetic Transition in Double-Exchange Systems. *J. Phys. Soc. Jpn.* **2001**, *70*, 1487–1490. [CrossRef]
22. Xi, S.B.; Lu, W.; Sun, Y. Magnetic properties and magnetocaloric effect of $La_{0.8}Ca_{0.2}MnO_3$ nanoparticles tuned by particle size. *J. Appl. Phys.* **2012**, *111*, 063922.
23. Khlifi, M.; Tozri, A.; Bejar, M.; Dhahri, E.; Hlil, E.K. Effect of calcium deficiency on the critical behavior near the paramagnetic to ferromagnetic phase transition temperature in $La_{0.8}Ca_{0.2}MnO_3$ oxides. *J. Magn. Magn. Mater.* **2012**, *324*, 2142–2146. [CrossRef]
24. Oesterreicher, H.; Parker, F.T. Magnetic cooling near Curie temperatures above 300 KJ. *Appl. Phys.* **1984**, *55*, 4334–4338. [CrossRef]
25. Franco, V.; Blazquez, J.S.; Conde, A. The magnetocaloric effect in soft magnetic amorphous alloys. *Appl. Phys. Lett.* **2006**, *89*, 222512. [CrossRef]
26. Turki, D.; Cherif, R.; Hlil, E.K.; Ellouze, M.; Elhalouani, F. The effect of Co doping on structural, magnetic and magnetocaloricproperties of $La_{0.8}Ca_{0.2}Mn_{1-x}Co_xO_3$ perovskites ($0 \leq x \leq 0.3$). *Int. J. Mod. Phys. B* **2014**, *28*, 1450230. [CrossRef]
27. Turki, D.; Remenyi, G.; Mahmood, S.H.; Hlil, E.K.; Ellouze, M.; Halouani, F. Magnetic contributions to the specific heat of $La_{0.8}Ca_{0.2}Mn_{1-x}Co_xO_3$ Perovskite. *Mater. Res. Bull.* **2016**, *84*, 245–253. [CrossRef]
28. Banerjee, S.K. On a generalised approach to first and second order magnetic transitions. *Phys. Lett.* **1964**, *12*, 16–17. [CrossRef]
29. Khlifi, M.; Bejar, M.; Dhahri, E.; Hlil, E.K. Preparation of New Composite Magnetocaloric Compounds by Modifying the Annealing Temperature of $La_{0.8}Ca_{0.2-x\Delta x}MnO_3$ Perovskite. *J. Supercond. Nov. Magn.* **2012**, *25*, 1151–1157. [CrossRef]
30. Lynn, J.W.; Erwin, R.W.; Borchers, J.A.; Huang, Q.; Santoro, A.; Peng, J.-L.; Li, Z.Y. Unconventional Ferromagnetic Transition in $La_{1-x}Ca_xMnO_3$. *Phys. Rev. Lett.* **1996**, *76*, 4046. [CrossRef] [PubMed]
31. Lin, P.; Chun, S.H.; Salamon, M.B.; Tomioka, Y.; Tokura, Y. Magnetic heat capacity in lanthanum manganite single crystals. *J. Appl. Phys.* **2000**, *87*, 5825–5827. [CrossRef]
32. Bonilla, C.M.; Albillos, J.H.; Bartolomé, F.; García, L.M.; Parra-Borderías, M.; Franco, V. Universal behavior for magnetic entropy change in magnetocaloric materials: An analysis on the nature of phase transitions. *Phys. Rev. B* **2010**, *81*, 224424. [CrossRef]
33. Kim, D.; Revaz, B.; Zink, B.L.; Hellman, F.; Rhyme, J.J.; Mitchell, J.F. Tricritical Point and the Doping Dependence of the Order of the Ferromagnetic Phase Transition of $La_{1-x}Ca_xMnO_3$. *Phys. Rev. Lett.* **2002**, *89*, 227202. [CrossRef] [PubMed]
34. Arrot, A.; Noakes, J.E. Approximate Equation of State For Nickel Near its Critical Temperature. *Phys. Rev. Lett.* **1967**, *19*, 786. [CrossRef]
35. Fan, J.; Ling, L.; Hong, B.; Zhang, L.; Pi, L.; Zhang, Y. Critical properties of the perovskite manganite $La_{0.1}Nd_{0.6}Sr_{0.3}MnO_3$. *Phys. Rev. B* **2010**, *81*, 144426. [CrossRef]
36. Kouvel, J.S.; Fisher, M.E. Detailed magnetic behavior of nickel near its curie point. *Phys. Rev.* **1964**, *43*, A1626. [CrossRef]
37. Zhang, L.; Fang, J.; Fan, J.; Ge, M.; Ling, L.; Zhang, C.; Pi, L.; Tan, S.; Zhang, Y. Critical behavior of the half-doped perovskite $Pr_{0.5}Sr_{0.5}CoO_{3-\Delta}$. *J. Alloys Compd.* **2014**, *588*, 294–299. [CrossRef]

38. Ghosh, K.; Lobb, C.J.; Greene, R.L.; Karabashev, S.G.; Shulyatev, D.A.; Arsenov, A.A.; Mukovskii, Y. Critical Phenomena in the Double-Exchange Ferromagnet $La_{0.7}Sr_{0.3}MnO_3$. *Phys. Rev. Lett.* **1998**, *81*, 4740. [CrossRef]
39. Jiang, W.; Zhou, X.Z.; Williams, G.; Mukovskii, Y.; Privezentsev, R. The evolution of Griffiths-phase-like features and colossal magnetoresistance in $La_{(1-x)}Ca_{(x)}MnO_{(3)}$ ($0.18 \leq x \leq 0.27$) across the compositional metal-insulator boundary. *J. Phys. Condens. Matter* **2009**, *21*, 415603. [CrossRef] [PubMed]
40. Thanh, T.D.; Linh, D.C.; Manh, T.V.; Ho, T.A.; Phan, T.; Yu, S.C. Coexistence of short- and long-range ferromagnetic order in $La_{0.7}Sr_{0.3}Mn_{1-x}Co_xO_3$ compounds. *J. Appl. Phys.* **2015**, *117*, 17C101. [CrossRef]
41. Phan, T.-L.; Ho, T.A.; Thang, P.D.; Tran, Q.T.; Thanh, T.D.; Phuc, N.X.; Phan, M.H.; Huy, B.T.; Yu, S.C. Critical behavior of Y-doped $Nd_{0.7}Sr_{0.3}MnO_3$ manganites exhibiting the tricritical point and large magnetocaloric effect. *J. Alloys Compd.* **2014**, *615*, 937–945.
42. Ho, T.A.; Phan, T.L.; Thang, P.D.; Yu, S.C. Influence of Pb doping on the Magnetocaloric Effect and Critical Behavior of $(La_{0.9}Dy_{0.1})_{0.8}Pb_{0.2}MnO_3$. *J. Electron. Mater.* **2016**, *45*, 2328–2333. [CrossRef]
43. Won, C.; Wu, Y.Z.; Arenholz, E.; Choi, J.; Wu, J.; Qiu, Z.Q. Symmetry-breaking induced exchange bias in ferromagnetics Ni-Cu-Co and Ni-Fe-Co sandwiches grown on vicinal Co (001) surface. *Phys. Rev. Lett.* **2007**, *99*, 77203. [CrossRef] [PubMed]
44. Widom, B. Surface Tension and Molecular Correlations near the Critical Point. *J. Chem. Phys.* **1964**, *41*, 163. [CrossRef]
45. Stanley, H.E. *Introduction to Phase Transitions and Critical Phenomena*; Oxford University Press: London, UK, 1971.
46. Khelifi, J.; Tozri, A.; Dhahri, E.; Hlil, E.K. Influence of Pr-doped manganite on critical behavior of $La_{0.7-x}Pr_xBa_{0.3}MnO_3$ (x = 0.00, 0.1, 0.2). *J. Magn. Magn. Mater.* **2014**, *349*, 149–155. [CrossRef]
47. Phan, T.L.; Min, S.G.; Yu, S.C.; Oh, S.K. Critical exponents of $La_{0.9}Pb_{0.1}MnO_3$ perovskite. *J. Magn. Magn. Mater* **2006**, *304*, e778–e780. [CrossRef]
48. Akahoshi, D.; Uchida, M.; Tomioka, Y.; Arima, T.; Matsui, Y.; Tokura, Y. Random Potential Effect near the Bicritical Region in Perovskite Manganites as Revealed by Comparison with the Ordered Perovskite Analogs. *Phys. Rev. Lett.* **2003**, *90*, 177203. [CrossRef] [PubMed]
49. Franco, V.; Conde, A. Magnetic refrigerants with continuous phase transitions: Amorphous and nanostructured materials. *Sci. Mater.* **2012**, *67*, 594–599. [CrossRef]
50. Franco, V.; Conde, A. Scaling laws for the magnetocaloric effect in second order phase transitions: From physics to applications for the characterization of materials, Lois d'échelle gouvernant l'effet magnétocalorique des transitions de phase de seconde ordre: De la physique aux applications permettant de caractériser les matériaux. *Int. J. Refriger.* **2010**, *33*, 465–473.
51. Caballero-Flores, R.; Franco, V.; Conde, A.; Dong, Q.Y.; Zhang, H.W. Study of the field dependence of the magnetocaloric effect in $Nd_{1.25}Fe_{11}Ti$: A multiphase magnetic system. *J. Magn. Mang. Mater.* **2010**, *322*, 804–807.
52. Nasri, M.; Triki, M.; Dhahri, E.; Hlil, E.K. Electrical transport and magnetoresistance properties of (1−x) $La_{0.6}Sr_{0.4}MnO_3$/x(Sb_2O_3) composites. *J. Alloys Compd.* **2013**, *576*, 404–408. [CrossRef]
53. Victorino, F.G.; Clara Francisca, C.A.; Javier Sebastián, B.G.; Alejandro, C.A.; Švec, P.; Janičkovič, D.; Kiss, F.L. A constant magnetocaloric response in FeMoCuB amorphous alloys with different FeB ratios. *J. Appl. Phys.* **2007**, *101*, 093903.
54. Prida, V.M.; Franco, V.; Vega, V.; S-Llamazares, J.L.; Sunol, J.J.; Conde, A.; Hernando, B. Magnetocaloric effect in melt-spun FePd ribbon alloy with second order phase transition. *J. Alloys Compd.* **2011**, *509*, 190–194. [CrossRef]
55. Shen, T.D.; Schwarz, R.B.; Coulter, J.Y.; Thompson, J.D. Magnetocaloric effect in bulk amorphous $Pd_{40}Ni_{22.5}Fe_{17.5}P_{20}Pd_{40}Ni_{22.5}Fe_{17.5}P_{20}$ alloy. *J. Appl. Phys.* **2002**, *91*, 5240–5245. [CrossRef]
56. Caballero-Flores, R.; Bingham, N.S.; Phan, M.H.; Torija, M.A.; Leighton, C.; Franco, V.; Conde, A.; L-Phan, T.; Yu, S.C.; Srikanth, H. Magnetocaloric effect and critical behavior in $Pr_{0.5}Sr_{0.5}MnO_3$: An analysis of the validity of the Maxwell relation and the nature of the phase transitions. *J. Phys. Condens. Matter* **2014**, *26*, 286001. [CrossRef] [PubMed]